

UC Berkeley

UC Berkeley Previously Published Works

Title

Ion diffusion across a disorder-to-order phase transition in a poly(ethylene oxide)- b - poly(silsesquioxane) block copolymer electrolyte

Permalink

<https://escholarship.org/uc/item/55736510>

Journal

Molecular Systems Design & Engineering, 4(2)

ISSN

2058-9689

Authors

Timachova, Ksenia
Sethi, Gurmukh K
Bhattacharya, Rajashree
[et al.](#)

Publication Date

2019-04-08

DOI

10.1039/c8me00077h

Peer reviewed

Ion diffusion across a disorder-order phase transition in a poly(ethylene oxide)-*b*-poly(silsesquioxane) block copolymer electrolyte

Ksenia Timachova^{†§}, Gurmukh Sethi^{□§}, Rajashree Bhattacharya[†], Irune Villaluenga[§], Nitash P. Balsara^{†§}

[†]Department of Chemical and Biomolecular Engineering, University of California, Berkeley, Berkeley, CA 94720, USA

[§]Materials Sciences Division and Joint Center for Energy Storage Research, Lawrence Berkeley National Laboratory, Berkeley, CA 94720, USA

[□]Department of Material Science and Engineering, University of California, Berkeley, Berkeley, CA 94720, USA

Nanostructured block copolymer electrolytes composed of organic and inorganic moieties have the potential to enable solid-state batteries. Practical uses of the materials, however, require an understanding of the microscopic and macroscopic ion transport properties across the microphase-separated systems. The self-diffusion of salt ions across a disorder-lamellar phase transition in a nanostructured poly(ethylene oxide)-*b*-poly(silsesquioxane) copolymer was studied using pulsed-field gradient NMR (PFG-NMR) and changes in the morphology were studied using small-angle x-ray scattering. The diffusion of the salt is isotropic when the polymer electrolyte is disordered and anisotropic when the polymer is microphase separated. The difference between the diffusion coefficient parallel to the lamellae, D_{\parallel} , and the diffusion coefficient perpendicular to the lamellae, D_{\perp} , measured using PFG-NMR increases above the phase transition and the two diffusivities diverge as the segregation strength increases with increasing temperature. The degree of anisotropy of diffusion increases with increasing

segregation strength, paralleling the changes in the morphology measured by small-angle x-ray scattering.

INTRODUCTION

Block copolymer electrolytes have the potential to enable solid-state batteries by providing independently tunable ion conduction and mechanical properties. The majority of experimental work in the field has focused on copolymers of organic molecules where one block preferentially solvates ions, while the other is mechanically rigid. The two blocks can phase separate into a variety of morphologies with features on the order of nanometers. These nanostructured morphologies have been well characterized both theoretically and experimentally.^{1,2} What is relevant to practical uses of these materials, however, is the relationship between nanoscale morphology and the dynamics of ion transport. Commonly, bulk conductivity measured on macroscopic samples is used as a metric of the efficacy of ion transport.³⁻⁸ Self-diffusion coefficients of the ions measured by pulsed-field gradient NMR provide insight into ion transport on more local length scales.⁹⁻¹¹

Helfand, Fredrickson, and coworkers have established a theoretical framework for understanding the diffusion of molecules across microphase separated block copolymers.¹²⁻¹⁷ Microphase block copolymer form ordered structures wherein coherent order is restricted to regions called grains. Molecular transport of a tracer molecule within individual grains is anisotropic for lamellar and cylindrical morphologies. Diffusion in these morphologies can be decoupled into the individual diffusivities along directions parallel and perpendicular to the interfaces between microphases. Building on that work, there have been a number of experimental investigations of diffusion aimed at measuring these distinct diffusion coefficients. Experimental studies on macroscopically aligned lamellar or

cylindrical samples have shown that the diffusion coefficient parallel to the lamellae or cylinders, D_{\parallel} , is larger than the perpendicular diffusion coefficient, D_{\perp} .¹⁸⁻²¹ Experimental work has shown that the average diffusion coefficient is continuous across the order-disorder transition.^{22,23} There are, however, no studies of the dependence of the diffusion coefficients D_{\parallel} and D_{\perp} on temperature across an order-disorder transition. In a related study, Majewski et al. measured ionic conductivity in the parallel and perpendicular directions in macroscopically aligned cylindrical block copolymer electrolytes across an order-disorder transition.²⁴

Polyhedral oligomeric silsesquioxanes (POSS) are silica nanoparticles with the empirical formula $\text{RSiO}_{1.5}$, where R is an organic functional group or hydrogen. POSS-containing block copolymers have been used in several applications including drug-delivery, battery electrolytes, and lithography templates.^{25,26} When combined with poly(ethylene oxide) (PEO), POSS has been used to make solid polymer electrolytes with star-shaped, brush-grafted, clustered, or crosslinked structures.²⁷⁻³¹ In his work, we use a PEO-POSS block copolymer mixed with a lithium salt to study ion transport across an disorder-order transition. We measure the parallel and perpendicular diffusion coefficients, D_{\parallel} and D_{\perp} , of the ions across the phase transition.

EXPERIMENTAL

Materials

Poly(ethylene oxide)-*b*-poly(silsesquioxane) with 5 kg/mol of PEO and 1 kg/mol of POSS (PEO-POSS(5-1)) was synthesized as described previously. **[Gumi paper]** The chemical structure of the block copolymer is shown in Fig. 1. Poly(ethylene oxide) with a molecular weight of 5 kg/mol (PEO(5)) was purchased from Polymer Source. Anhydrous tetrahydrofuran (THF) and benzene were purchased from Sigma-Aldrich, and lithium

bis(trifluoromethanesulfonyl)imide salt, Li[N(SO₂CF₃)₂] (LiTFSI), was purchased from Novolyte. PEO-POSS(5-1) was dried at 90°C under vacuum in the glovebox antechamber for 48 h before use. PEO-POSS(5-1)/LiTFSI electrolyte with a molar ratio of lithium atoms to ethylene oxide (EO) monomers, $r = 0.1$, was made by dissolving dry polymer and LiTFSI into anhydrous THF and mixing at 60°C for a minimum of 12 h. Once dissolved, the THF was evaporated by drying the solution on a hotplate at 90°C for 48 h. The remaining polymer/salt mixture was additionally dried under vacuum for 48 h at 90°C to remove all residual solvent.

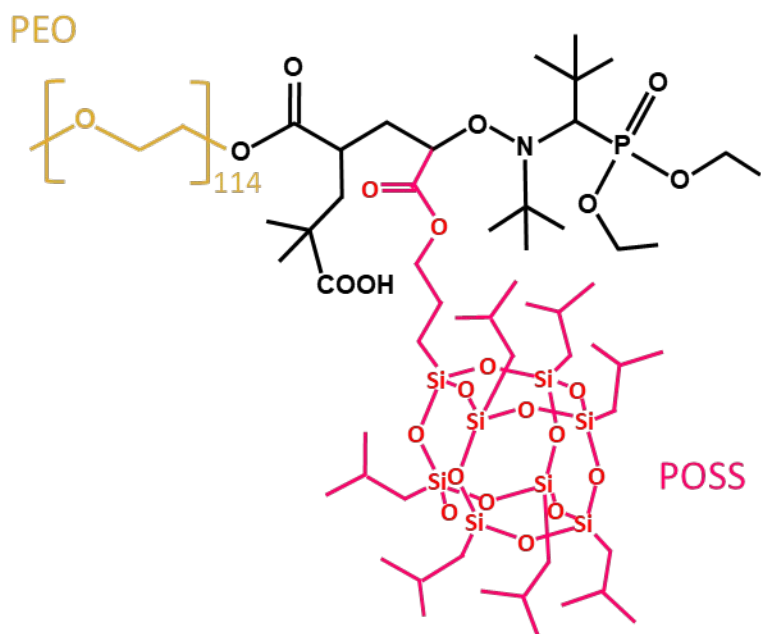


Figure 1. Chemical structure of the PEO-POSS block copolymer.

Small-angle X-ray Scattering

The morphology of the electrolyte was determined by small-angle x-ray scattering (SAXS). The SAXS sample was prepared by pressing the electrolyte at 90°C into 1 mm thick rubber spacers with a 1/8 in. inner-diameter and sealed with Kapton windows in custom-designed airtight holders. The samples were annealed at 110°C under vacuum for at least 24

h. Measurements were performed at beamline 1-5 at the Stanford Synchrotron Radiation Lightsource (SSRL) at SLAC National Accelerator Laboratory. Samples were mounted in a custom-built heating stage and held at each temperature for at least 30 min before measurement. Silver behenate was used to determine the beam center and sample-to-detector distance. The scattered intensity was corrected for beam transmission. Two-dimensional scattering patterns were integrated azimuthally using the Nika program³² for Igor Pro to produce one-dimensional scattering profiles and are reported as scattering intensity, I , as a function of the magnitude of the scattering vector, $q = 4\pi\sin\theta/2\lambda$ where θ is the scattering angle, and λ is the wavelength of the x-rays equal to 1.2398 Å. The samples were heated from room temperature to the highest temperature of 143°C in approximately 20°C increments and cooled in 10°C increments.

Pulsed-Field Gradient NMR

All NMR samples were packed into 5 mm tubes in an argon-filled glovebox and sealed with high pressure caps. Diffusion measurements were performed on a Bruker Avance-600 spectrometer fitted with a broadband probe and variable temperature unit. Single peaks were observed for ⁷Li and ¹⁹F at 233 MHz and 565 MHz, respectively, corresponding to all Li- and TFSI-containing species. A stimulated echo bipolar gradient pulse sequence with one orthogonal spoiler gradient pulse was used to measure diffusion. Gradient pulse lengths, $\delta = 0.5-16$ ms and diffusion times, $\Delta = 0.4-3$ s were used. The gradient strength g was linearly increased with 32 values steps from 0.7 up to 33 G/cm.

The equation for anisotropic diffusion in planar structures is^{11,33}

$$I = I_0 \frac{1}{2} \int_0^\pi \exp(-\dots) d\alpha$$

where I is the intensity of the signal, I_0 is the initial intensity at low gradient strength, γ is the gyromagnetic ratio, δ is the length of the gradient pulse, g is the strength of the gradient pulse, Δ is the diffusion time, and θ is an integration angle, corresponding to all the possible orientations of the nanostructure with respect to the gradient axis. In order to expedite the fitting algorithm, a modified diffusion decay equation was used to fit the data. Eq. 1 can be simplified to

$$I = I_0 \frac{1}{2} \exp(-\dots)$$

where $erfi$ is the imaginary error function. Eq. 1 and Eq. 2 are mathematically equivalent, but eq. 2 is easier to compute using iterative minimization algorithms and provides for faster and better fits to D_{\parallel} and D_{\perp} . All data was fit to eq. 2 with the constraint $D_{\parallel} > D_{\perp}$ using a nonlinear least-squares algorithm.

RESULTS

Azimuthally averaged small-angle x-ray scattering profiles of PEO-POSS(5-1)/LiTFSI at $r = 0.1$ over a range of temperatures are shown in Fig. 2(a). The broad peak at $q = 0.28 \text{ nm}^{-1}$ at temperatures below 105°C , gives way to two peaks at q^* and $2q^*$ at temperatures above 105°C indicating a disorder-to-order transition. A disordered morphology is present below 102°C shown in Fig. 2(c) and a lamellar phase is present at temperatures above 112°C shown in Fig. 2(b). We note that the scattering profiles of disordered PEO-POSS(5-1) are different from those obtained in conventional block copolymers.³⁴ This may be due to the high density of Si atoms present in the POSS that is expected to dominate the scattering intensity.

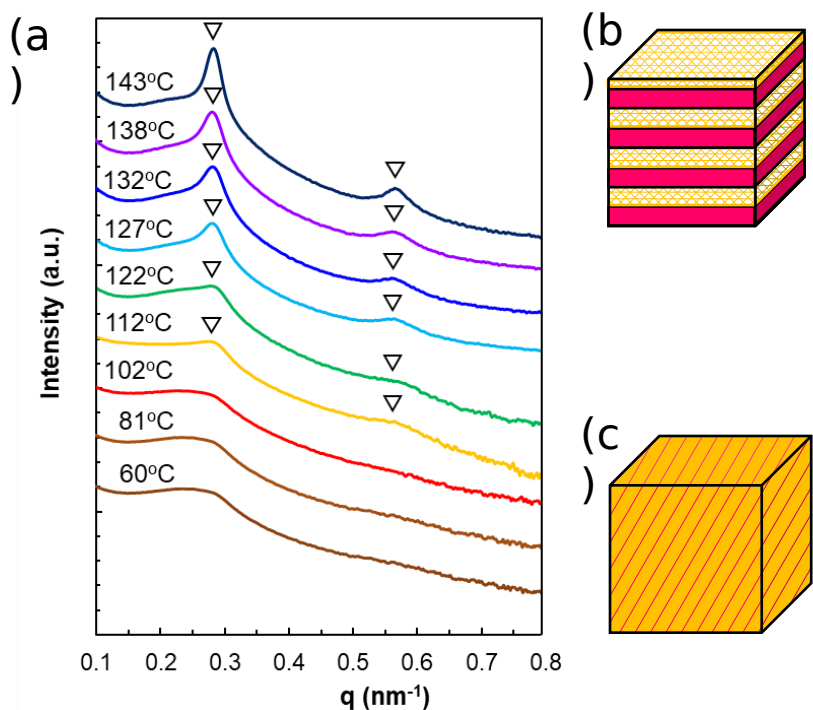


Figure 2. (a) Azimuthally averaged small-angle x-ray scattering intensity of PEO-POSS(5-1)/LiTFSI with $r = 0.1$ as a function of scattering vector, q , and temperature. Triangles (∇) indicate the location of the primary (q^*) and second order ($2q^*$) peaks corresponding to a lamellar morphology. Depictions of (b) lamellar and (c) disordered morphologies.

The diffusion of Li and TFSI was measured by PFG-NMR in PEO-POSS(5-1) at $r = 0.1$ over a range of temperatures encompassing both disordered and ordered morphologies. The decays of the PFG-NMR signals due to diffusion of Li and TFSI are shown in Fig. 3 on a log-linear scale. Diffusion at 100°C, a temperature in the disordered state right below the disorder-order transition is shown in Fig. 3(a) and (b). The diffusion decays of both Li and TFSI at 100°C exhibit single exponential behavior, indicative of isotropic diffusion. Diffusion decays at 140°C, a temperature in the ordered state above the disorder-order transition, are shown in Fig. 3(c) and (d). The dashed lines in Fig. 3 are linear fits through the first 16 data points in each decay. Departures between the data and the linear fits are clearly seen at 140°C.

The diffusion decays of both Li and TFSI are not single-exponentials at 140°C, indicative of anisotropic diffusion within lamellae.^{11,33} There is more scatter in the Li data due to the lower signal-to-noise of ⁷Li NMR relative to ¹⁹F.

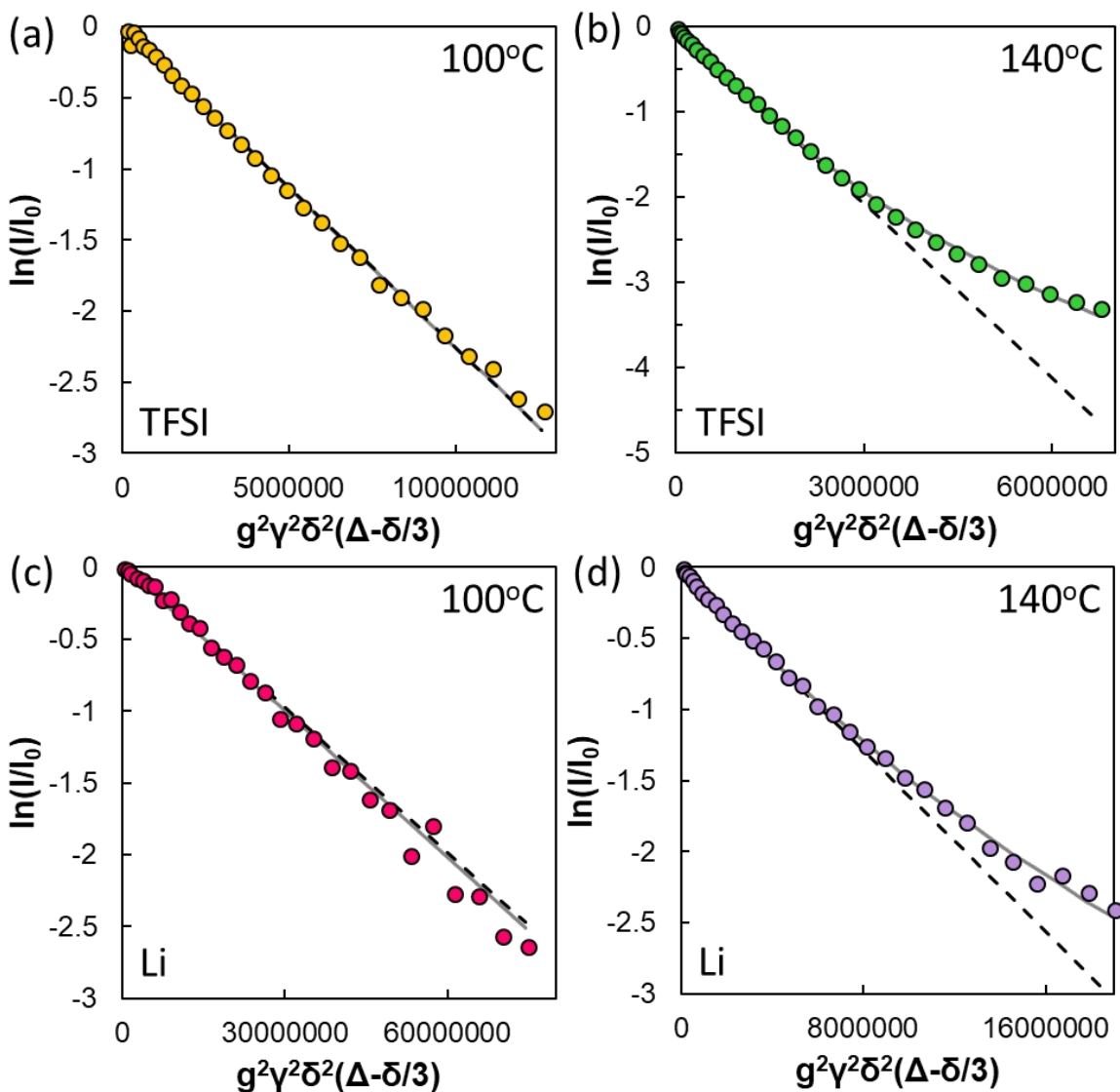


Figure 3. Diffusion decays in PEO-POSS (5-1) of (a) ¹⁹F at 100°C, (b) ¹⁹F at 140°C, (c) ⁷Li at 100°C, and (d) ⁷Li at 140°C. To show deviation from single exponential behavior, linear fits to the first 16 points of the data are shown as dotted black lines. Actual fits to the data using eq. 2 are shown as solid grey lines.

The data in Fig. 3 were fit to eq. 2 with D_{\parallel} and D_{\perp} as adjustable parameters, where D_{\parallel} is the diffusion coefficient of the ions parallel to the lamellae and D_{\perp} is the diffusion coefficient of the ions perpendicular to the lamellae. This fitting procedure was used for all temperatures below and above the disorder-order transition, to obtain the temperature dependence of D_{\parallel} and D_{\perp} . The fits for the data shown in Fig. 3, are shown as solid grey lines. Diffusion coefficients D_{\parallel} and D_{\perp} of Li and TFSI for the range of temperatures 90-140°C are shown in Fig. 4. The overlap in D_{\parallel} and D_{\perp} at low temperatures indicates the presence of a single isotropic diffusion coefficient. This is true at 90°C and 100°C for both the Li and TFSI, where the block copolymer is disordered. At temperatures above the disorder-order transition, D_{\parallel} and D_{\perp} begin to diverge, and the difference between D_{\parallel} and D_{\perp} increases with increasing temperature. At 140°C, deep in the ordered state, D_{\parallel} for Li is larger than D_{\perp} by a factor of 10.

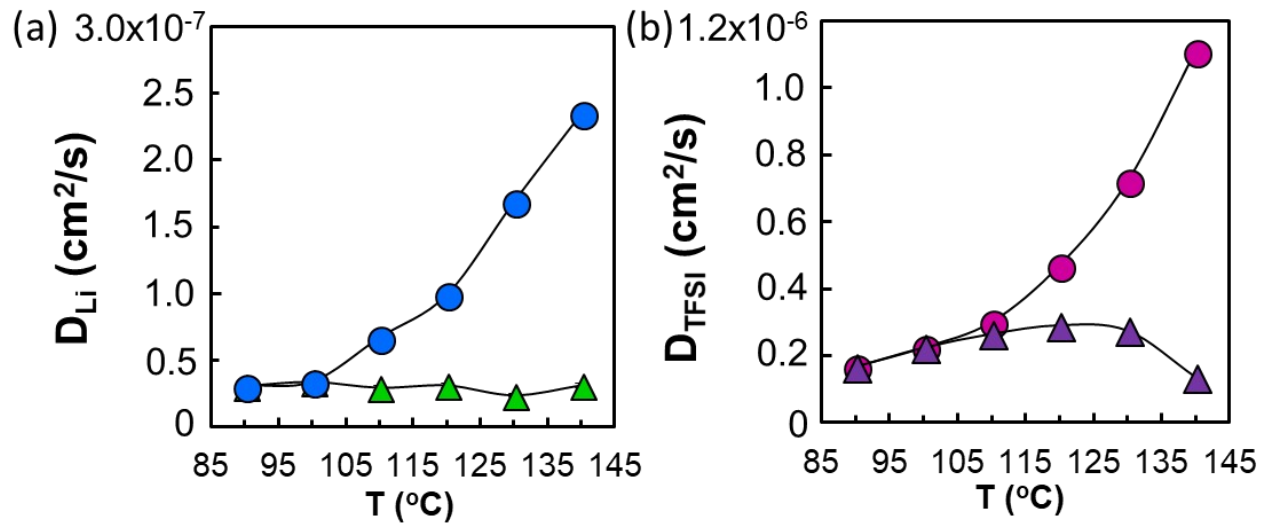


Figure 4. Diffusion coefficients of (a) Li and (b) TFSI parallel to and perpendicular to the lamellae.

In Fig. 4, D_{\parallel} and D_{\perp} depend both on temperature and on the morphology of the block copolymer. Our main interest is to focus on the dependence of the diffusion coefficients on morphology. We define reduced diffusion coefficients D_{\parallel}/D_{PEO} and D_{\perp}/D_{PEO} where D_{PEO} is the diffusion coefficient of Li and TFSI measured in homopolymer poly(ethylene oxide) (PEO(5)) at the same value of temperature and r . The Li and TFSI diffusivities in PEO(5) are plotted as a function of temperature in the insets of Fig. 5. The reduced diffusivities D_{\parallel}/D_{PEO} and D_{\perp}/D_{PEO} are plotted in Fig. 5.

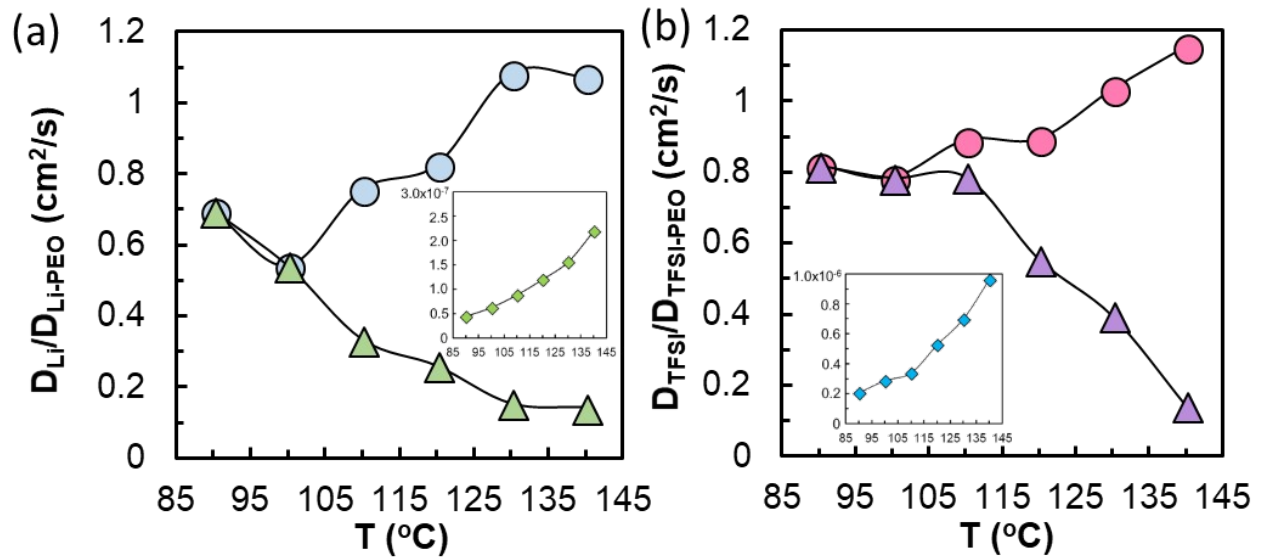


Figure 5. Reduced diffusion coefficients, D_{\parallel}/D_{PEO} and D_{\perp}/D_{PEO} , of the (a) Li and (b) TFSI parallel to and perpendicular to the lamellae as a function of temperature. The diffusion coefficient of (a) Li and (b) TFSI measured in homopolymer poly(ethylene oxide) (PEO(5)), D_{PEO} , at the same value of temperature and r is shown in the insets.

The reduced diffusion coefficients, D_{\parallel}/D_{PEO} and D_{\perp}/D_{PEO} for Li and TFSI, shown in Fig. 5(a) and (b) are less than one in the disordered state. We attribute this to interactions between the Li and TFSI ions and the POSS block in

disordered PEO-POSS(5-1). Above the disorder-order transition, D_{\parallel}/D_{PEO} increases with increasing segregation, approaching a value of around one at high temperatures. In the ordered state, Li and TFSI ions are confined to PEO-rich lamellae in PEO-POSS(5-1). As segregation increases, the POSS monomers are increasingly excluded from the PEO-rich lamellae and diffusion within the lamellae, D_{\parallel} , is indistinguishable from diffusion in PEO homopolymer of the same molecular weight, D_{PEO} . Concomitantly, as segregation increases, the PEO monomers are increasingly excluded from the POSS-rich lamellae and diffusion through the POSS microphase is hindered. This is seen in the dramatic decrease of the reduced diffusion coefficient perpendicular to the lamellae, D_{\perp}/D_{PEO} , with increasing segregation in Fig. 5. D_{\perp}/D_{PEO} approach values as low as 0,1 at 140°C.

A second order peak seen at $q = 2q^*$ in Fig. 2(a) is a standard signature of an ordered lamellar phase. The magnitude of this second order peak was used to quantify the degree of phase segregation. The area under the second order peak in the was calculated by subtracting an exponential baseline from the spectra in Fig. 2(a) in the vicinity of $2q^*$ and integrating the resulting scattering intensity. At temperatures below 102°C, the area of the $2q^*$ peak is negligible, indicating a disordered morphology. At temperatures above 112°C, the area of the $2q^*$ peak increases with increasing temperature reflecting an increase in the segregation between PEO and POSS monomers in adjacent lamellae. The disorder-order transition occurs between 102°C and 112°C.

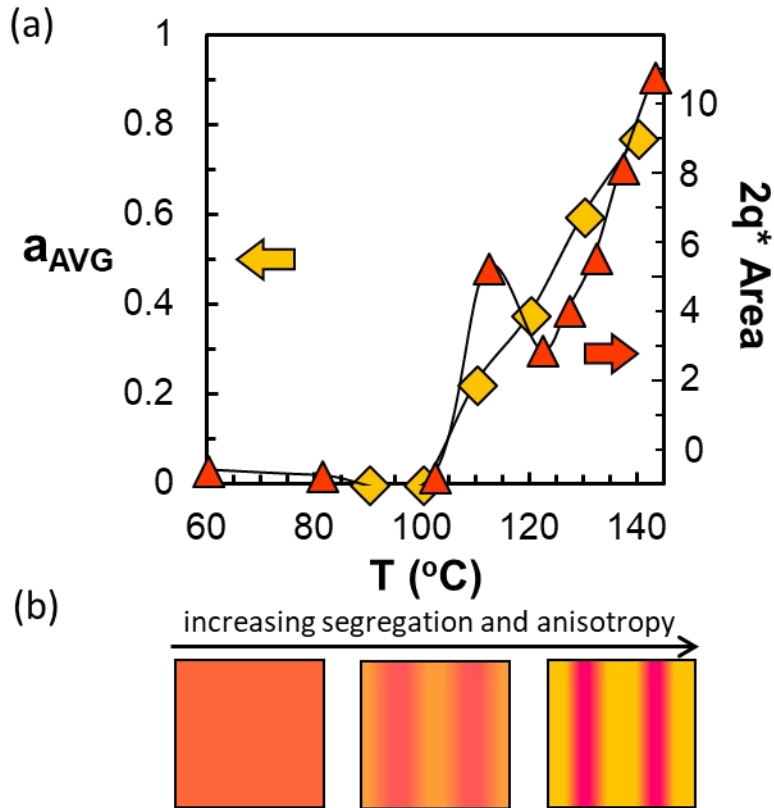


Figure 6. (a) The integrated area under the second order SAXS peak, $2q^*$, (triangles, right axis) and the calculated average degree of diffusion anisotropy, a_{AVG} , (diamonds, left axis) from ^7Li and ^{19}F diffusion in PEO-POSS(5-1) as a function of temperature. (b) Schematic of the segregation between PEO and POSS blocks as a function of temperature.

A commonly used parameter to quantify anisotropic diffusion is a ^{35,36}

$$a = \frac{D_{i\parallel} - D_{i\perp}}{D_{i\parallel} + D_{i\perp}}$$

We define a_{AVG} as the average value of a for Li and TFSI, $a_{\text{AVG}} = (a_{\text{Li}} + a_{\text{TFSI}})/2$. For isotropic diffusion, $a=0$. If diffusion is perfectly anisotropic and no ions move perpendicular to the lamellae, $a=1$. The average degree of anisotropy a_{AVG} is also plotted in Fig. 6(a). It is clear that in the disordered state below both a_{AVG} is zero and the area under the second order peak is negligible. At the temperatures above the disorder-order phase transition, the polymer

becomes microphase segregated as shown in Fig. 6(b), and both a_{AVG} and the area under the second order peak increase. Diffusion anisotropy is closely correlated with the segregation strength.

CONCLUSION

The self-diffusion of Li and TFSI ions across a disorder-lamellar phase transition in a PEO-POSS block copolymer was studied using SAXS and PFG-NMR. The polymer-salt system exhibits a disorder-to-order transition between 102°C and 112°C; it is disordered below 102°C and ordered above 112°C. The diffusion coefficients of the ions are isotropic when the system is disordered, while locally anisotropic diffusion is observed in the ordered state. The difference between the diffusion parallel to the lamellae, D_{\parallel} , and the diffusion perpendicular to the lamellae, D_{\perp} , increases with increasing temperature in the ordered state, paralleling the increase in segregation strength determined measured by SAXS.

AUTHOR INFORMATION

Corresponding Authors

*Nitash Balsara, E-mail: nbalsara@berkeley.edu

Author Contribution

The manuscript was written through contributions of all authors. All authors have given approval to the final version of the manuscript.

ACKNOWLEDGEMENTS

This work was intellectually led by the Joint Center for Energy Storage Research (JCESR), an Energy Innovation Hub funded by the U.S. Department

of Energy (DOE), Office of Science, Basic Energy Sciences (BES), under Contract No. DEAC02-06CH11357.

REFERENCES

- (1) Bates, F. S.; Fredrickson, G. H. Block Copolymer Thermodynamics: Theory and Experiment. *Annual Review of Physical Chemistry* **1990**, *41* (1), 525–557.
- (2) Bates, F. S.; Fredrickson, G. H. Block Copolymers—Designer Soft Materials. *Physics Today* **2008**, *52* (2), 32.
- (3) Bouchet, R.; Phan, T. N. T.; Beaudoin, E.; Devaux, D.; Davidson, P.; Bertin, D.; Denoyel, R. Charge Transport in Nanostructured PS-PEO-PS Triblock Copolymer Electrolytes. *Macromolecules* **2014**, *47* (8), 2659–2665.
- (4) Chintapalli, M.; Le, T. N. P.; Venkatesan, N. R.; Mackay, N. G.; Rojas, A. A.; Thelen, J. L.; Chen, X. C.; Devaux, D.; Balsara, N. P. Structure and Ionic Conductivity of Polystyrene-Block-Poly(Ethylene Oxide) Electrolytes in the High Salt Concentration Limit. *Macromolecules* **2016**, *49* (5), 1770–1780.
- (5) Ganesan, V.; Pyramitsyn, V.; Bertoni, C.; Shah, M. Mechanisms Underlying Ion Transport in Lamellar Block Copolymer Membranes. *ACS Macro Lett.* **2012**, *1* (4), 513–518.
- (6) Lobitz, P.; Füllbier, H.; Reiche, A.; Illner, J. C.; Reuter, H.; Höring, S. Ionic Conductivity in Poly (Ethylene Oxide)-Poly (Alkylmethacrylate)-Block Copolymer Mixtures with Lil. *Solid State Ionics* **1992**, *58* (1–2), 41–48.
- (7) Mullin, S. A. *Morphology and Ion Transport in Block-Copolymer Electrolytes*; University of California, Berkeley, 2011.
- (8) Wanakule, N. S.; Panday, A.; Mullin, S. A.; Gann, E.; Hexemer, A.; Balsara, N. P. Ionic Conductivity of Block Copolymer Electrolytes in the Vicinity of Order–Disorder and Order–Order Transitions. *Macromolecules* **2009**, *42* (15), 5642–5651.
- (9) Bhattacharja, S.; Smoot, S. W.; Whitmore, D. H. Cation and Anion Diffusion in the Amorphous Phase of the Polymer Electrolyte (PEO) 8LiCF₃SO₃. *Solid State Ionics* **1986**, *18*, 306–314.
- (10) Hayamizu, K.; Akiba, E.; Bando, T.; Aihara, Y. ¹H, ⁷Li, and ¹⁹F Nuclear Magnetic Resonance and Ionic Conductivity Studies for Liquid Electrolytes Composed of Glymes and Polyetheneglycol Dimethyl Ethers of CH₃O(CH₂CH₂O)_NCH₃ (N=3–50) Doped with LiN(SO₂CF₃)₂. *The Journal of Chemical Physics* **2002**, *117* (12), 5929–5939.
- (11) Timachova, K.; Villaluenga, I.; Cirrincione, L.; Gobet, M.; Bhattacharya, R.; Jiang, X.; Newman, J.; Madsen, L. A.; Greenbaum, S. G.; Balsara, N. P. Anisotropic Ion Diffusion and Electrochemically Driven Transport in

- Nanostructured Block Copolymer Electrolytes. *J. Phys. Chem. B* **2018**, *122* (4), 1537–1544.
- (12) Helfand, E. Diffusion in Strongly Segregated Block Copolymers. *Macromolecules* **1992**, *25* (1), 492–493.
- (13) Fredrickson, G. H.; Bates, F. S. Dynamics of Block Copolymers: Theory and Experiment. *Annu. Rev. Mater. Sci.* **1996**, *26* (1), 501–550.
- (14) Fredrickson, G. H. Tracer-Diffusion in Quenched Lamellar Phases. *Acta Polymerica* **1993**, *44* (2), 78–82.
- (15) Fredrickson, G. H.; Milner, S. T. Tracer-Diffusion in Weakly-Ordered Block Copolymers. *MRS Online Proceedings Library Archive* **1989**, 177.
- (16) Barrat, J. L.; Fredrickson, G. H. Diffusion of a Symmetric Block Copolymer in a Periodic Potential. *Macromolecules* **1991**, *24* (24), 6378–6383.
- (17) Leibig, C. M.; Fredrickson, G. H. Tracer Diffusion in Fluctuating Block Copolymer Melts. *Journal of Polymer Science Part B: Polymer Physics* **1996**, *34* (1), 163–171.
- (18) Kannan, R. M.; Su, J.; Lodge, T. P. Effect of Composition Fluctuations on Tracer Diffusion in Symmetric Diblock Copolymers. *The Journal of Chemical Physics* **1998**, *108* (11), 4634–4639.
- (19) Hamersky, M. W.; Tirrell, M.; Lodge, T. P. Anisotropy of Diffusion in a Lamellar Styrene–Isoprene Block Copolymer. *Langmuir* **1998**, *14* (24), 6974–6979.
- (20) Hamersky, M. W.; Hillmyer, M. A.; Tirrell, M.; Bates, F. S.; Lodge, T. P.; von Meerwall, E. D. Block Copolymer Self-Diffusion in the Gyroid and Cylinder Morphologies. *Macromolecules* **1998**, *31* (16), 5363–5370.
- (21) Ehlich, D.; Takenaka, M.; Okamoto, S.; Hashimoto, T. FRS Study of the Diffusion of a Block Copolymer. 1. Direct Determination of the Anisotropic Diffusion of Block Copolymer Chains in a Lamellar Microdomain. *Macromolecules* **1993**, *26* (1), 189–197.
- (22) Shull, K. R.; Kramer, E. J.; Bates, F. S.; Rosedale, J. H. Self-Diffusion of Symmetric Diblock Copolymer Melts near the Ordering Transition. *Macromolecules* **1991**, *24* (6), 1383–1386.
- (23) Hamersky, M. W.; Tirrell, M.; Lodge, T. P. Self-Diffusion of a Polystyrene-Polyisoprene Block Copolymer. *Journal of Polymer Science Part B: Polymer Physics* **1996**, *34* (17), 2899–2909.
- (24) Majewski, P. W.; Gopinadhan, M.; Jang, W.-S.; Lutkenhaus, J. L.; Osuji, C. O. Anisotropic Ionic Conductivity in Block Copolymer Membranes by Magnetic Field Alignment. *J. Am. Chem. Soc.* **2010**, *132* (49), 17516–17522.
- (25) Hussain, H.; Tan, B. H.; Seah, G. L.; Liu, Y.; He, C. B.; Davis, T. P. Micelle Formation and Gelation of (PEG–P(MA-POSS)) Amphiphilic Block Copolymers via Associative Hydrophobic Effects. *Langmuir* **2010**, *26* (14), 11763–11773.
- (26) Hirai, T.; Leolukman, M.; Liu, C. C.; Han, E.; Kim, Y. J.; Ishida, Y.; Hayakawa, T.; Kakimoto, M.; Nealey, P. F.; Gopalan, P. One-Step Direct-

- Patterning Template Utilizing Self-Assembly of POSS-Containing Block Copolymers. *Advanced Materials* **2009**, *21* (43), 4334–4338.
- (27) Zhang, J.; Ma, C.; Liu, J.; Chen, L.; Pan, A.; Wei, W. Solid Polymer Electrolyte Membranes Based on Organic/Inorganic Nanocomposites with Star-Shaped Structure for High Performance Lithium Ion Battery. *Journal of Membrane Science* **2016**, *509*, 138–148.
- (28) Kim, S.-K.; Kim, D.-G.; Lee, A.; Sohn, H.-S.; Wie, J. J.; Nguyen, N. A.; Mackay, M. E.; Lee, J.-C. Organic/Inorganic Hybrid Block Copolymer Electrolytes with Nanoscale Ion-Conducting Channels for Lithium Ion Batteries. *Macromolecules* **2012**, *45* (23), 9347–9356.
- (29) Lee, J. Y.; Lee, Y. M.; Bhattacharya, B.; Nho, Y.-C.; Park, J.-K. Solid Polymer Electrolytes Based on Crosslinkable Polyoctahedral Silsesquioxanes (POSS) for Room Temperature Lithium Polymer Batteries. *Journal of Solid State Electrochemistry* **2010**, *14* (8), 1445–1449.
- (30) Polu, A. R.; Rhee, H.-W. Nanocomposite Solid Polymer Electrolytes Based on Poly(Ethylene Oxide)/POSS-PEG (N=13.3) Hybrid Nanoparticles for Lithium Ion Batteries. *Journal of Industrial and Engineering Chemistry* **2015**, *31*, 323–329.
- (31) Yu, C.-B.; Ren, L.-J.; Wang, W. Synthesis and Self-Assembly of a Series of NPOSS-b-PEO Block Copolymers with Varying Shape Anisotropy. *Macromolecules* **2017**, *50* (8), 3273–3284.
- (32) Ilavsky, J. Nika: Software for Two-Dimensional Data Reduction. *Journal of Applied Crystallography* *45* (2), 324–328.
- (33) Wang, Z.; Gobet, M.; Sarou-Kanian, V.; Massiot, D.; Bessada, C.; Deschamps, M. Lithium Diffusion in Lithium Nitride by Pulsed-Field Gradient NMR. *Physical Chemistry Chemical Physics* **2012**, *14* (39), 13535.
- (34) Mori, K.; Hasegawa, H.; Hashimoto, T. Small-Angle X-Ray Scattering from Bulk Block Polymers in Disordered State. Estimation of χ -Values from Accidental Thermal Fluctuations. *Polymer Journal* **1985**, *17* (6), 799–806.
- (35) Moseley, M. E.; Cohen, Y.; Kucharczyk, J.; Mintorovitch, J.; Asgari, H. S.; Wendland, M. F.; Tsuruda, J.; Norman, D. Diffusion-Weighted MR Imaging of Anisotropic Water Diffusion in Cat Central Nervous System. *Radiology* **1990**, *176* (2), 439–445.
- (36) Li, J.; Park, J. K.; Moore, R. B.; Madsen, L. A. Linear Coupling of Alignment with Transport in a Polymer Electrolyte Membrane. *Nat Mater* **2011**, *10* (7), 507–511.